PHYSICAL REVIEW B VOLUME 59, NUMBER 7 15 FEBRUARY 1999-I

Electronic structure and magnetism of Rh_n ($n=2-13$) clusters

B. V. Reddy, S. K. Nayak, S. N. Khanna, B. K. Rao, and P. Jena
Department of Physics, Virginia Commonwealth University, Richmond, Virginia 23284-2000

(Received 27 July 1998)

Theoretical studies of the ground-state geometries, electronic structure, binding energies, ionization potentials, and magnetic moments of Rh_n ($n=2-13$) clusters have been carried out using a combination of molecular-dynamics and *ab initio* density-functional scheme including gradient corrections. For clusters containing less than eight atoms, the ground states have been determined by starting from several random configurations and minimizing the geometry using first-principles density-functional calculations. For larger clusters, the initial geometries were obtained via molecular-dynamics simulations based on a tight-binding many-body potential and reoptimized using the density-functional approach. The ground-state structures are all compact arrangements and the clusters containing 8, 9, 10, 11, and 12 atoms resemble icosahedral fragments. The clusters are shown to undergo progression of magnetic behaviors with size. While most clusters are ferromagnetic with varying magnetic moments, Rh_4 and Rh_6 are found to have nonmagnetic states that are nearly degenerate with ferromagnetic states. The variation in the magnetic moments is shown to be intimately linked to the electronic structure. [S0163-1829(99)06207-4]

I. INTRODUCTION

The developments in experimental methods over the past few years have enabled scientists to generate, characterize, and study clusters of any size and composition.[1] These studies have revealed that clusters are a state of matter with their own distinct properties. Some of the most exciting developments are in the field of magnetism where the properties have been found to change profoundly as one reduced the size from bulk to clusters. For example, clusters of itinerant ferromagnetic elements Fe, Co, and Ni have been found to exhibit superparamagnetic relaxations[2] while clusters of rare-earth ferromagnets like Gd show canted spin arrangements.[3] The most striking development is the possibility of clusters of nonmagnetic solids to be magnetic.[4–6] Calculations[4] on nonmagnetic elements such as vanadium have shown that their clusters with bulk geometry are magnetic. However, it is the experimental evidence of magnetism of small Rh clusters[6] that has given new life to the study of magnetism of atomic clusters. It is important to emphasize that the experimental work of Cox and co-workers[6] followed the theoretical prediction by Reddy, Khanna, and Dunlap[5] that Rh_{13} is magnetic. The measured moment of Rh_{13} was, however, smaller than the predicted value. These experiments also showed that the magnetic moments change nonmonotonically with size and that the ferromagnetic character disappears as the cluster size approached around 100 atoms.

Following the above work there have been several attempts to study Rh_n clusters theoretically using different methods.[7–9] We will summarize these results in the next section. It is sufficient at this stage to note that all theoretical works on Rh_n clusters where the geometries have been optimized are restricted to $n \leqslant 6$ while the experiment deals with clusters $n \geqslant 9$. Some calculations[7] for Rh_n clusters containing 8, 10, 12, 13, and 19 atoms are available, but the geometries of these clusters were fixed from the start. Since the magnetic properties of Rh clusters depend sensitively on their geometry,[8] one cannot draw any quantitative comparison between this theory[7] and experiment.[6]

In this paper we provide an in-depth study of the ground-state geometry, binding energy, electronic structure, and magnetic moments of Rh_n clusters containing between 2 and 13 atoms. We compare our results with previous calculations for $n \leqslant 6$ and provide results on optimized geometries for $6 < n \leqslant 13$ for the first time. Our studies are based on a combination of *ab initio* molecular orbital theory and molecular dynamics using realistic interatomic potentials. The key focus of the current work is the magnetic behavior. We show that the magnetic moments vary nonmonotonically with size and several clusters exhibit magnetically close multiplets. The later are shown to be intimately linked to the details of the electronic spectra. Section II contains details of the method and in Sec. III we give our results. Section IV contains the main conclusions of the present study.

II. DETAILS OF CALCULATIONS

The theoretical studies were carried out using a combination of *ab initio* linear combination of atomic orbitals molecular-orbital (LCAO-MO) and molecular-dynamics simulation with a realistic potential. For clusters containing less than eight atoms, the calculations were carried out using the molecular-orbital approach within the density-functional scheme. The cluster wave functions are expressed as a linear combination of atomic orbitals centered at the atomic sites. The atomic orbitals are taken in a numerical form and are obtained via a radial solution of the atomic Schrödinger equation on a mesh of points. The basis sets for Rh included $4s$, $4p$, $4d$, and $5s$ orbitals in addition to $5p$ polarization functions. The inner core orbitals ($1s-3d$) were frozen. The computations were carried out using the DMOL (Ref. 10) code from Biosym technologies. As we will show later, some clusters are marked by close multiplet states. In these cases, we have also carried out selected studies by using the GAUSSIAN 94 software[11] where the atomic orbitals are represented by Gaussian functions. A comparison of results obtained using DMOL and GAUSSIAN 94 codes can illustrate the dependence of results on the choice of basis functions and the numerical procedure. The Gaussian studies used LANL2DZ basis proposed by Hay and Wadt.[12] In all cases, the exchange correlation effects were included by using either the local-spin-density approximation (LSDA) or the generalized gradient approximation (GGA). We used the local-density functionals of Vosko, Wilk, and Nusair[13] and the GGA functional proposed by Perdew and Wang.[14]

For clusters containing more than seven atoms, the *ab initio* determinations of the ground-state structures become computationally difficult because of a large number of possible local minima in the total energy hypersurface. In these cases, we have used a hybrid approach combining molecular-dynamics (MD) and *ab initio* methods. Our experience with MD using realistic many body potentials[15] has shown that while the MD does lead to correct ordering of various isomers, the bond lengths using many body potentials can be different from those in an *ab initio* calculation. We have, therefore, used the following approach. Using realistic many-body potentials,[16] we investigate the relative stability of a large number of structures by carrying out MD calculations. For the most stable geometry, the bond lengths were then reoptimized using the *ab initio* code maintaining the symmetry of the MD structure.

In this work we have used the tight-binding many-body potential proposed by Guevara, Llois, and Weissmann.[16] The parameters entering the potential were obtained by fitting the cohesive energy, bulk modulus, and surface relaxation of bulk Rh and the binding energy of the dimer. To confirm that the MD simulation does provide meaningful starting geometries for optimizing the geometries of larger $(n>7)$ clusters, we compare in Fig. 1 the geometries, bond lengths, and binding energies for Rh_n $(n\leqslant 7)$ clusters obtained independently from *ab initio* theory and MD simulations. Note that the ground-state geometries obtained from MD simulations are the same as those derived from *ab initio* calculations except for the case of Rh_5. For Rh_5, we have found two nearly degenerate isomers. In the molecular orbital calculations the square pyramid is 0.07 eV/atom more stable than the triangular bipyramid while in the MD method the triangular bipyramid is 0.08 eV/atom more stable than the square pyramid structure. These energy differences are small and the two isomers can be regarded as nearly degenerate in energy. Note, however, that the bond lengths between the local-density functional (DFT) and MD structures are somewhat different in all clusters indicating that further optimization of the MD bond length is needed at the *ab initio* level.

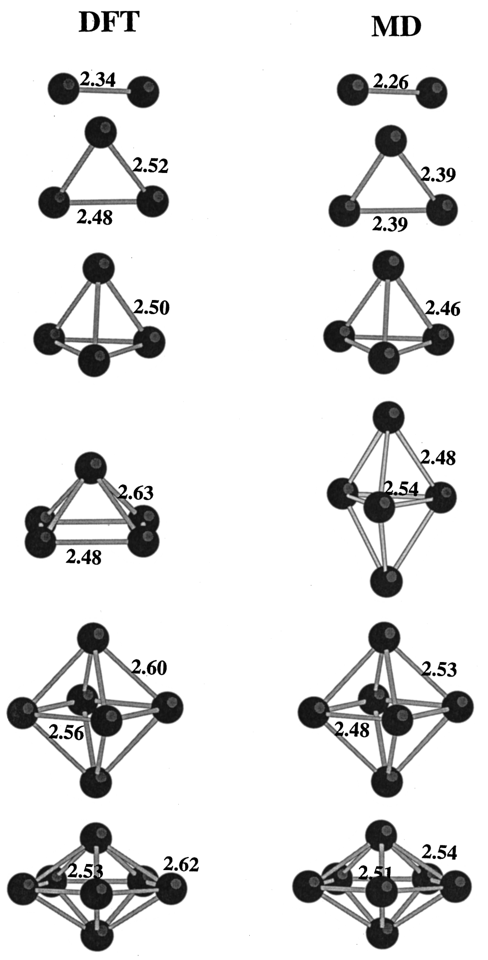

FIG. 1. Ground-state geometries of small Rh_n $(n\leqslant 7)$ clusters obtained by using the *ab initio* and MD simulations.

The constant energy MD simulations were carried out by integrating the Newton's equations of motion using a Verlet algorithm with a time step of $3\times 10^{-15}\,\mathrm{s}$.[17] The total energy was conserved to within 0.01% and the angular and linear momentum were kept at zero at the start of each calculation. For each cluster, typically around 100 initial configurations were used and the structures optimized by using the steepest descent method. The structures were ordered in terms of their energy and the most stable structures were heated and recooled to generate the final most stable structure. Starting from the ground-state structure obtained in the MD simulations, the bond lengths were reoptimized at the *ab initio* level maintaining the symmetry of the MD structure. Note that the many-body potential does not contain any spin-dependent term, but the reoptimization at the *ab initio* level does. In the *ab initio* calculations, various spin states were examined to determine the final ground state and the corresponding electronic structure and spin multiplicity.

III. RESULTS AND DISCUSSION

This section is divided into various subsections: In A we provide a summary of previous theoretical work on Rh_n $(n\leqslant 6)$ clusters and compare these with our results. We also discuss the evolution of the geometries and relative stability of larger, Rh_n $(n\geqslant 7)$ clusters. The evolution of the structural and electronic properties as well as the binding energy and the fragmentation pattern of these clusters are analyzed in subsection B. The main focus of this work, namely, the magnetic properties of Rh clusters $(n\geqslant 7)$, is covered in subsection C.

A. Equilibrium geometries of Rh_n $(n\leqslant 13)$ clusters and comparison with earlier works

We start with the Rh atom. The experimental ground state of the atom is ^4F $(4d^8 5s^1)$ with 5↑ and 3↓ electrons in the $4d$ orbital. Using the numerical frozen core basis in the

TABLE I. Comparison of the present results on Rh_2 with previous calculations and experiment.

Calculations Authors	Method	Bond length (Å)	B.E./atom (eV)	Spin multiplicity $(2S+1)$
Shim (Ref. 18)	CI	2.86	0.43	5
Balasubramanian and Liao (Ref. 19)	CI	2.28	1.05	5
Illas *et al.* (Ref. 20)	CI	2.67	0.75	5
Jinlong and co-workers (Ref. 7)	LDA	2.31	1.52	5
Harada & Dexpert (Ref. 21)	GGA	2.56		5
Chien, Blaisten-Barojas, and Pederson (Ref. 9)	GGA	2.33	1.38	5
Nayak *et al.* (Ref. 8)	GGA	2.26	1.51	5
Present	GGA	2.34	1.88	5
Expt. (Ref. 22)		2.28	1.46	5

DMOL code, we obtain the ground state to be ^2D both at the LSDA and generalized gradient approximation (GGA) level of theory. However, this state is 0.68 eV above the ^4F state. Other authors[9] have also obtained the ^2D state as the ground state of the atom. We have examined this problem with the Gaussian 94 code using the effective core potential. Here, however, we do find the Rh atom to have the correct ground state, namely, $4d^8 5s^1$. The ^2D state, in this case, lies only 0.002 eV higher in LSDA and 0.12 eV in GGA than the ground state. The energy differences, thus, are very small and, as we shall see later, do not influence the results on the Rh clusters. We also calculated the first ionization potential. The calculated value of 7.97 eV within the GGA using the DMOL code is comparable to the experimental value of 7.46 eV. We now present our results on clusters and compare them to the previous calculations and experiment.

In Table I, we compare our calculated binding energy, bond length, and spin multiplicity for Rh_2 and also make comparisons with previous theoretical works[7–9,18–21] and experiment.[22] Note that the calculated binding energy/atom ranges over a wide margin with very low binding in configuration interaction (CI) calculations to over binding in density-functional studies. This behavior is typical. It is, however, discomforting that the binding energy obtained by Jinglong and co-workers[7] using LSDA is lower than our present GGA value based on the DMOL code. It is well known that LSDA gives rise to overbinding. In this context, we should point out that the discrete variational method used by Jinglong and co-workers is a predecessor to the DMOL code used here and Nayak *et al.*[8] have already discussed the possible origin of the discrepancy with the work of Jinglong and co-workers.[7] All calculations, irrespective of their method and approximations, yield the preferred spin multiplicity to be 5, i.e., $2\mu_B$/atom.

The results on Rh_3 (Refs. 7–9, 24, 25) are summarized in Table II. Unlike the results of Rh_2 where all calculations yield a spin quintet ground state, Rh_3 has two magnetically degenerate states: a spin quartet configuration where Rh_3 is an equilateral triangle (D_{3h}) and a spin sextet configuration where its geometry is that of an isosceles triangle (C_{2v}). The long bond (2.52 Å) and short bond (2.48 Å) of the sextet state agree well with other calculations based on the GGA. While the C_{2v} structure, both in the present calculations and in those of Chien, Blaisten-Barojas, and Pederson[9] calculations, is marginally lower than the D_{3h} symmetry, the reverse is the case with the calculations by Nayak *et al.*[8] However, the energy differences between these structures are so small (0.01–0.05 eV/atom) that, within the accuracy of the

TABLE II. Comparison of the present results on Rh_3 with previous calculations.

Calculations Authors	Method	Symmetry	Bond lengths (Å)	B.E./atom (eV)	Spin multiplicity $(2S+1)$
Jinlong and co-workers (Ref. 7)	LDA	C_{2v}	2.46, 2.46, 2.34	2.26	4
Das & Balasubramanian (Ref. 24)	CI	C_{2v}	2.53, 2.53, 2.60	2.72	4
Dai & Subramanian (Ref. 25)	CI	C_{2v}	2.60, 2.60, 2.23	3.59	6
Chien, Blaisten-Barojas,	GGA	C_{2v}	2.64, 2.64, 2.44	1.95	6
and Pederson (Ref. 9)		D_{3h}	2.42	1.94	
Nayak	GGA	C_{2v}	2.53, 2.53, 2.40	1.94	6
et al. (Ref. 8)		D_{3h}	2.42	1.99	4
Present	GGA	C_{2v}	2.52, 2.52, 2.48	2.37	6
		D_{3h}	2.45	2.35	4

TABLE III. Comparison of the present results on Rh_4 with previous calculations.

Calculations Authors	Method	Geometry	Bond lengths (Å)	B.E./atom (eV)	Spin multiplicity $(2S+1)$
Jinlong and co-workers (Ref. 7)	LSDA	tetrahedron	2.48	2.95	1
Chien, Blaisten-Barojas, and Pederson (Ref. 9)	GGA	tetrahedron	2.50	2.42	1
		square	2.39	2.37	5
Nayak *et al.* (Ref. 8)	GGA	tetrahedron	2.49	2.41	1
		square	2.38	2.35	5
Present	GGA	tetrahedron	2.50	2.91	1
		square	2.40	2.79	5

theoretical procedure, it is hard to argue whether if C_{2v} or D_{3h} is the actual ground state. We should recall that the Rh atom's ground state was properly given by the calculations of Nayak *et al.*[8] There are no experiments on the ground-state spin structure of Rh_3 cluster in the gas phase. However, electron spin resonance[23] experiments on Rh_3 clusters prepared in argon/krypton matrices indicate a multiplicity of 6 or 8. In Table II we also compare our calculations with previous studies[24,25] based on multireference configuration interaction calculations. Dai and Balasubramanian[25] find three nearly degenerate C_{2v} sextet states with binding energies and bond lengths differing by 0.03 eV/atom and 0.05 Å, respectively. While we are unable to comment on the significance of these values, we find the binding energy/atom obtained by these authors to be particularly large in comparison to that of the Rh_2 calculated by them earlier.[19]

Rh_4 is the smallest cluster that could assume a three-dimensional structure. Consequently, we optimized the geometry subject to a three dimensional D_{2d} as well as a planar D_{2h} symmetry. The ground state is a tetrahedron with a bond length of 2.50 Å and a binding energy of 2.91 eV/atom (Fig. 1). It is a spin singlet. Rh_4 is therefore the smallest Rh_n cluster to have a nonmagnetic ground state. We also found a square geometry only 0.12 eV/atom above the ground state but having a spin quintet multiplicity. These results agree with the calculations of Chien, Blaisten-Barojas, and Pederson[9] and Nayak *et al.*[8] (Table III). This aspect of the result, which shows an interesting relation between geometry and multiplicity, will be discussed later.

For Rh_5, we studied the triangular bipyramid and the square pyramid geometries. In each case, the geometry was optimized for various spin multiplicities. The ground state corresponds to a square pyramid with bond lengths of 2.48 and 2.63 Å as shown in Fig. 1. It has a binding energy of 3.11 eV/atom and a spin octet configuration. (see Table IV). The sextet state is only 0.02 eV/atom above the ground state with the corresponding bond lengths of 2.46 and 2.57 Å. The ground state for the triangular bipyramid was a quartet. However, this structure is 0.35 eV less stable than the square pyramid structure. This again shows that the ground-state multiplicity in Rh_n clusters is intimately linked to geometry. Note that the present ground state is not in agreement with previous calculations by Jinlong and co-workers,[7] but agrees with the results of Chien, Blaisten-Barojas, and Pederson.[9]

We examined the square bipyramid and the pentagonal pyramid geometries for Rh_6. The ground state is a square bipyramid with a D_{4h} symmetry (Fig. 1). It has bond lengths of 2.60 and 2.56 Å, a binding energy of 3.28 eV/atom and a spin singlet configuration. The septet configuration is found to be 0.01 eV/atom less stable than the ground state. Note that the energy difference is very small. The results again demonstrate the existence of different spin multiplet structures with nearly degenerate energies. While the structure examined by Chien, Blaisten-Barojas, and Pederson[9] had an O_h symmetry, we find that the octahedron undergoes a small Jahn-Teller distortion and only has a D_{4h} symmetry. Interestingly, the local-spin-density calculations on O_h symmetry also find a nonmagnetic ground state.

For Rh_7 we examined a pentagonal bipyramid and capped octahedron clusters. In each case, the possible Jahn-Teller distortions were investigated. The ground state corresponds to a distorted pentagonal bipyramid with a binding energy of 3.33 eV/atom and a spin multiplicity of 10 (see Fig. 1). This structure lies 0.02 eV/atom below the capped octahedron structure.

As mentioned in Sec. II, for clusters containing more than seven atoms, the number of isomers becomes large and *ab initio* studies of all possible geometries and spin multiplici-

TABLE IV. Comparison of the present calculations on Rh_5 with previous work.

Author	Bond lengths (Å)	B.E./atom (eV)	Spin multiplicity $(2S+1)$
Chien, Blaisten-Barojas, and Pederson (Ref. 9)	2.65,3.44	2.70	6
	2.66,3.50	2.69	8
Present	2.46,2.57	3.11	6
	2.48,2.63	3.13	8

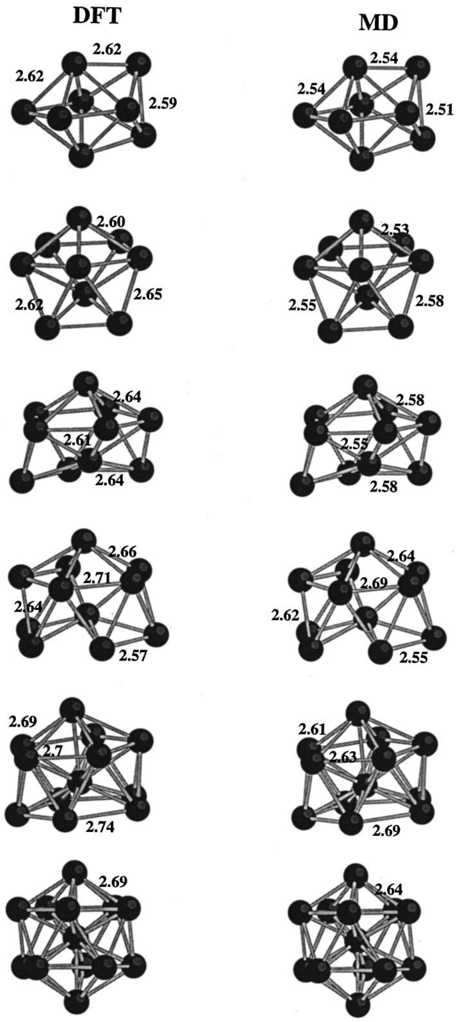

FIG. 2. Ground-state geometries for large Rh_n ($n=8-13$) clusters.

ties is a computationally formidable task. We therefore determined the initial structures using MD simulations. Starting from such a structure, the bond lengths were optimized retaining the lowest symmetry at the *ab initio* level within the density-functional calculations.

In Fig. 2 we show the ground-state geometries of the clusters containing 8–13 atoms. The ground state for Rh_8 is a D_{2d} structure that resembles an octahedron with two decorated faces. For Rh_9, the top six atoms constitute a fragment of an icosahedron. This pattern continues to Rh_{11}, which has two pentagons of the eventual icosahedron. Rh_{12} is the smallest cluster to have a central atom and is an icosahedron with a missing cap atom. Finally, Rh_{13} has an icosahedric structure.

B. Evolution of the structural and electronic properties and fragmentation pattern

Here we discuss the evolution of the interatomic distance, binding energy/atom, highest occupied molecular orbital–lowest unoccupied molecular orbital (HOMO-LUMO) gap, vertical ionization potential, and the fragmentation pattern of Rh_n ($n\leq 13$) clusters. Since the interatomic distances vary

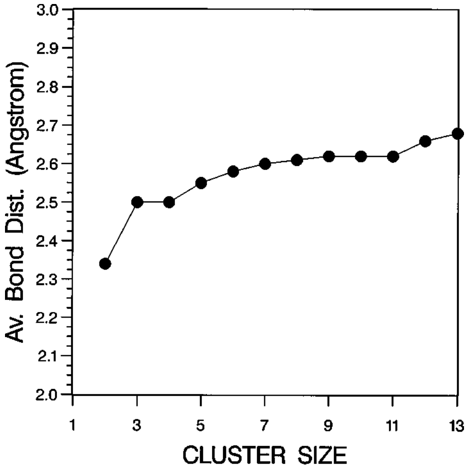

FIG. 3. Average interatomic distance as a function of cluster size.

between nearest-neighbor atoms in each of these clusters, we define the average interatomic distance, $\bar{R}=(1/n)\Sigma_i R_i$, where i defines the number of bonds in the cluster having a length of R_i. In Fig. 3 we plot $\bar{R}$ as a function of cluster size, n. Note that the average interatomic distance increases monotonically with size, and for $n=13$, is comparable to the bulk nearest-neighbor distance of 2.69 Å.

In Fig. 4 we plot the binding energy/atom. It increases monotonically with size although the rate of increase decreases with size. It is difficult to predict from Fig. 4 if certain clusters of Rh are more stable than others as has been clearly demonstrated for simple metal clusters such as the alkali series. To study if any of these Rh clusters could be magic, we investigated the fragmentation pattern of these clusters. It is well known that when a cluster containing n atoms undergoes a binary fragmentation to m and (n-m) clusters, the dominant channel involves the most stable cluster as one of the daughter products.[26] To investigate this, we have calculated the energy needed to fragment n-atom cluster to m and (n-m) atoms, namely

$$\Delta E_{nm}=E_{n-m}+E_m-E_n \qquad (1)$$

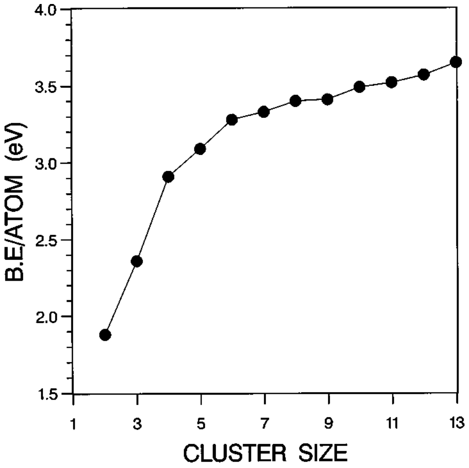

FIG. 4. Plot of binding energy vs cluster size.

TABLE V. Fragmentation channels for a n atom cluster into a m and a n-m atom cluster.

n	m	1	2	3	4	5	6	7	8	9	10	11	12
2		3.76											
3		3.34	3.34										
4		4.55	4.13	4.55									
5		3.91	4.70	4.70	3.91								
6		4.12	4.27	5.48	4.27	4.12							
7		3.63	3.99	4.56	4.56	3.99	3.63						
8		3.89	3.76	4.54	3.90	4.54	3.76	3.89					
9		3.49	3.62	3.91	3.48	3.48	3.91	3.62	3.49				
10		4.21	3.94	4.49	3.57	3.78	3.57	4.49	3.94	4.21			
11		3.82	4.27	4.42	3.76	3.48	3.48	3.76	4.42	4.27	3.82		
12		4.12	4.18	5.05	3.99	3.97	3.48	3.97	3.99	5.05	4.18	4.12	
13		4.61	4.97	5.45	5.11	4.69	4.46	4.46	4.69	5.11	5.45	4.97	4.61

where E_n is the total energy of a cluster of n atoms. For a given n, the favored channel is the one for which ΔE_{nm} is the minimum. In Table V we give the results of this analysis. Note that for $n \geqslant 7$, the most favored channel for fragmentation involves Rh_6. This would cause Rh_6 to be a uniquely stable cluster and should appear as a magic number in the mass spectrum. This prediction can be easily verified when the mass spectra of Rh clusters are available. Note also that the binding energy per atom in a Rh_{13} cluster is only 3.67 eV/atom, which is far short of the cohesive energy of 5.75 eV/atom in bulk Rh. The lower binding energy is expected since Rh_{13} has 12 surface atoms. On the other hand, as noted earlier, the nearest-neighbor distance of Rh_{13} is bulklike.

In Fig. 5 we show our calculated vertical ionization potentials for these clusters. The clusters containing 2–4 atoms have significantly higher ionization potentials. For other clusters, the ionization potential gradually decreases with size, although there are minor oscillations around Rh_8. The ionization potential of Rh_{13} is 5.83 eV and is still higher than the work function for bulk Rh, which is 4.98 eV. There are currently no available experimental data on ionization potential of small Rh clusters.

In Fig. 6 we plot the HOMO-LUMO gap as a function of cluster size. The HOMO-LUMO gap shows an interesting trend. It is very small for Rh_2 and Rh_3 with a very sharp increase in Rh_4 followed by a gradual decrease in larger clusters. This is in contrast to Ni_n clusters,[27] where the HOMO-LUMO gap uniformly decreases with an increase in size and vanishes at $n = 17$, indicating the onset of the bulklike density of states. This is in agreement with the photoelectron spectroscopy experiments of Ni clusters. No such experiments are available in Rh_n clusters at this time. Clearly, it will be interesting to compare these results with experiments when available.

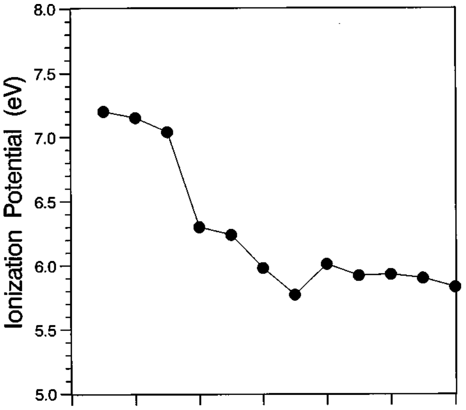

FIG. 5. Plot of vertical ionization potential as a function of cluster size.

C. Magnetic moments of Rh_n clusters

As mentioned in the Introduction, the most interesting property of Rh clusters is that while bulk Rh is paramagnetic, small Rh_n clusters exhibit ferromagnetic order. Experiments[6] show that the magnetic moment per atom in Rh clusters changes nonmonotonically with size. It is also known that the introduction of ferromagnetic impurities such as Fe in bulk Rh induces large host polarization. All of these facts suggest that the Rh clusters may serve as an ideal system to understand the interplay between size, geometry, electronic structure, and magnetism.

In Fig. 7 we plot the calculated magnetic moment (solid circles) per atom as a function of cluster size. The measured

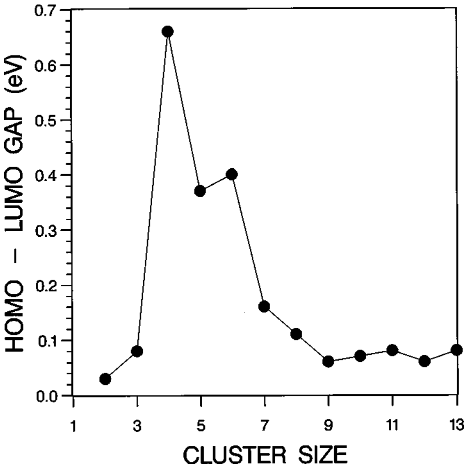

FIG. 6. HOMO-LUMO gap vs cluster size.

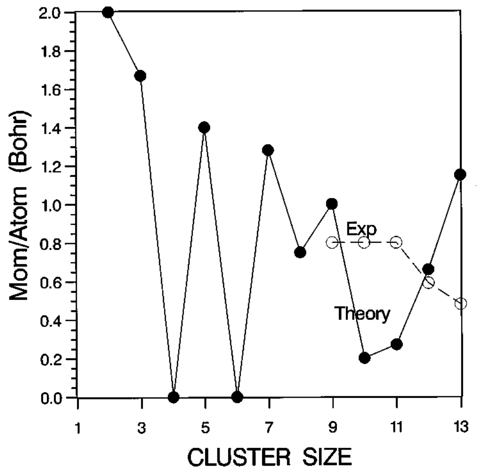

FIG. 7. Variation of magnetic moments (μ_B/atom) as a function of cluster size.

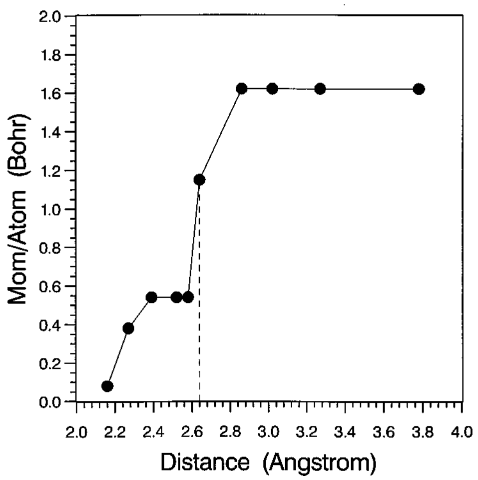

FIG. 9. Variation of magnetic moment vs interatomic distance in Rh_{13} icosahedron cluster.

moments are shown as open circles. Note that the magnetic moment changes discontinuously with size and Rh_4 is the smallest cluster to exhibit a nonmagnetic ground state. Its ground state geometry is a D_{2d} structure. The cluster also exhibits a magnetic solution with a moment of 1.0 μ_B/atom, where the geometry is a square. To understand this change in the magnetic moment with geometry we show in Fig. 8 the one-electron levels in a tetrahedral and a square geometry. Note that the HOMO in a tetrahedral geometry is full and the lowest unoccupied molecular orbital LUMO is separated by almost 0.66 eV. As the structure changes to a square geometry, the changes in electronic structure cause two of the LUMO states to come closer to HOMO. It is then energetically favorable to transfer two electrons from the minority states to the majority states so that the gain in exchange energy is higher than the kinetic energy needed to occupy the higher-energy states. The cluster therefore changes to a quintet spin multiplicity.

The change in magnetic moment not only occurs because of a change in the geometry but can also be induced by a change in bond length that changes the spacing between levels. The case of Rh_{13} presents an interesting example. In Fig. 9 we have shown the variation of the magnetic moment in a Rh_{13} cluster as a function of interparticle spacing. Note that the magnetic moment at large distances is $21\mu_B$. As the interparticle distance is reduced, the moment changes to $15\mu_B$ at a distance of approximately 2.6 Å (which is energetically the preferred structure) and then shows another plateau at $7\mu_B$. Upon further contraction, it reduces to a very small value. It is interesting that these progressions can be related to the distribution of levels in the one electron spectrum. In Fig. 10 we show the one electron levels for the clusters having magnetic moments of 7, 15, and $21\mu_B$. Starting from the $7\mu_B$ structure, the HOMO has a fivefold degeneracy but only has one electron. As the interparticle spacing is increased, the bandwidth decreases due to decreasing overlap, and at a distance of 2.65 Å, the level spacing is such that the gain in exchange energy due to transfer of four electrons from the minority states to fill the majority levels is more

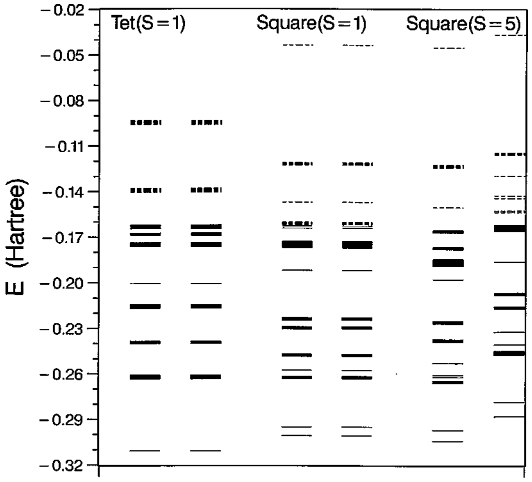

FIG. 8. Plot showing one-electron levels of a Rh_4 cluster. See the text for details.

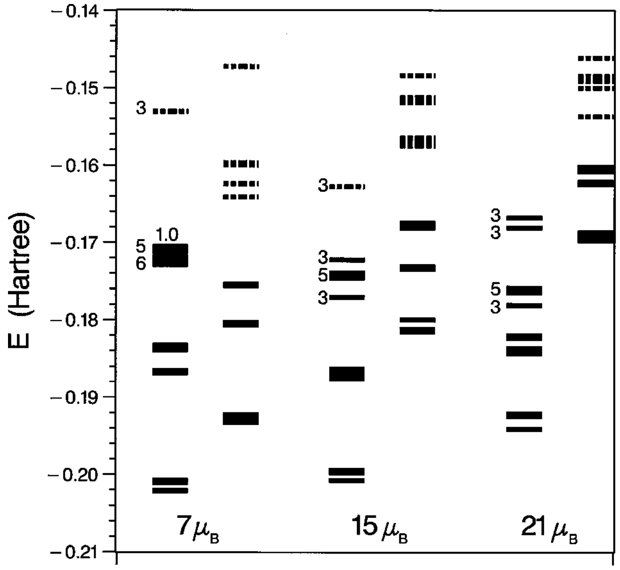

FIG. 10. One electron levels of Rh_{13} cluster for different magnetic states.

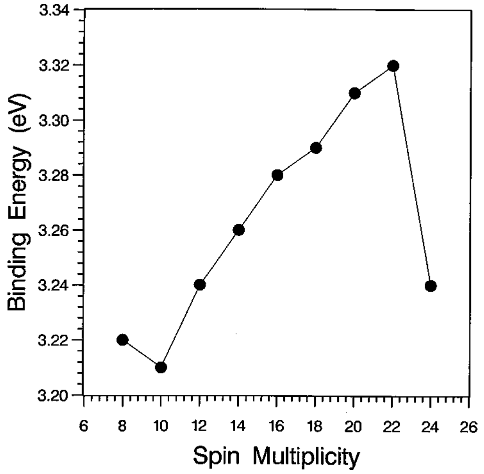

FIG. 11. Variation of binding energy as a function of magnetic moments in the Rh_{13} cluster.

than the energy required to promote electrons to higher energy states, and the cluster undergoes an increase of moment by $8.0\mu_B$. The majority spin levels have another set of unoccupied triply degenerate levels close to HOMO. Further increase in interparticle spacing leads to a transfer of three additional minority electrons to the majority level increasing the spin to $21\mu_B$. The total energy of the system, however, has a minimum at 2.65 Å and therefore the ground state of a Rh_{13} cluster has a moment of $1.15\mu_B$/atom. Dunlap[28] has earlier observed this dependence of moment on interatomic separation in Fe clusters.

We now compare our calculated magnetic moments with experiment. As mentioned before, Reddy, Khanna, and Dunlap[5] had earlier carried out density-functional calculations using LSDA on a Rh_{13} cluster and had found that the cluster had a moment of $1.62\mu_B$/atom. Initial experiments, while confirming the ferromagnetism in clusters, found a moment of $0.88\pm0.16\mu_B$/atom. Following the experimental work, Jinlong and co-workers[7] repeated the calculations and found a solution corresponding to a moment of $1.15\mu_B$/atom to be more stable than that corresponding to a moment of $1.62\mu_B$/atom by 0.35 eV. In the present studies including gradient correction, we do find the state with a moment of $1.15\mu_B$/atom (total spin moment of 15) to be the more stable than that corresponding to $1.62\mu_B$/atom by approximately 0.25 eV. We would like to add that this energy difference ($\sim$25 meV/atom) is too small and at the limit of the accuracy of the current density-functional calculations. For example, we repeated Rh_{13} calculations using the Gaussian basis and Gaussian 94 code. The ground state corresponds to a spin moment of $21\mu_B$. In Fig. 11 we have shown the binding energy per atom for spin moments from 7 to $23\mu_B$. Note that the binding energy changes by less than 0.1 eV/atom as the moment is changed from 7 to $23\mu_B$, showing that different multiplets are really close in energy. Similar results in the cases of Rh_4 and Rh_6 clusters were discussed earlier. We also found, for Rh_3, a state with a spin moment of $1.0\mu_B$/atom only 0.007 eV/atom above the ground state, which has a moment of $1.67\mu_B$/atom. Rh_5 has a state with a moment of $1.0\mu_B$/atom only 0.02 eV/atom above the ground state, which has a moment of $1.4\mu_B$/atom. All these examples illustrate that the Rh clusters are marked by several multiplet solutions close to the ground states.

The experimental magnetic moments (open circles) are compared with theoretical results in Fig. 7. Note that while the calculated moments are close to experiment for Rh_9 and Rh_{12}, there are significant differences for clusters having 10, 11, and 13 atoms. There could be several reasons for these differences. (1) Various isomers of a given Rh cluster exhibit a multitude of spin multiplicities. Since these are energetically nearly degenerate, they could all simultaneously be present in the experimental beam. Thus, the deflection of a given cluster in the Stern-Gerlach field is difficult to interpret since the deflection depends on its magnetic moment and each isomer has a different magnetic moment. This may be the reason for the large experimental uncertainty in the measurements of the moments of Rh clusters compared to similar experiments in Fe, Co, and Ni.[29] (2) The intrinsic moment in the experiment is determined by relating the deflection in the magnetic field via the superparamagnetic equation, which requires a knowledge of the cluster vibrational temperature. Knowledge of the cluster temperature is a difficult task and has always been a source of controversy.[29] (3) In addition, since the clusters are always at finite temperature, it is possible that they are not in their ground state, particularly if the ground state has energetically close excited states. (4) We have neglected possible contributions from orbital magnetism as well as spin-orbit coupling. It will be interesting to have additional experiments which can eliminate some of the current uncertainties.

IV. CONCLUSIONS

We have presented an in-depth investigation of the geometries, electronic structure and magnetic moment of Rh_n clusters. It is shown that the geometries of small clusters are compact structures which evolve towards an icosahedric geometry starting, at approximately seven atoms. Rh_{12} is the first cluster to have an interior atom. The binding energy per atom evolves monotonically with size. However, energetics of the fragmentation channels indicates that Rh_6 could be a ''magic'' cluster. The binding energy/atom of the largest cluster studied, Rh_{13}, is far from the bulk cohesive energy although its nearest-neighbor distance has achieved the bulk value. The HOMO-LUMO gaps show unusual features not seen in other transition-metal clusters. The magnetic character and the magnetic moment per atom are found to vary nonmonotonically with size. Rh_2 and several odd atom clusters, i.e., Rh_3, Rh_5, Rh_7, Rh_9, and Rh_{13} have high moments per atom and are ferromagnetic. On the other hand, Rh_4 and Rh_6 have nonmagnetic ground states that are nearly degenerate with magnetic configurations. The clusters are also shown to be marked by energetically close multiple magnetic solutions. For the cases of Rh_4 and Rh_{13}, it is shown that the different multiplicity can be attained by changing the geometry or the interparticle spacing. Further, these changes can be understood in terms of the variations in the electronic states.

ACKNOWLEDGMENTS

The authors are grateful to the Department of Energy (Contract No. DE-FG02-96ER45579) for financial support.

[1] *Proceedings of the Sixth International Conference of Small Particles and Inorganic Clusters* [Z. Phys. D **26** (1993)].

[2] S. N. Khanna and S. Linderoth, Phys. Rev. Lett. **67**, 742 (1991).

[3] D. P. Pappas, A. P. Popov, A. N. Anisimov, B. V. Reddy, and S. N. Khanna, Phys. Rev. Lett. **76**, 4332 (1996).

[4] D. R. Salahub and R. P. Messmer, Surf. Sci. **106**, 415 (1981); F. Liu, S. N. Khanna, and P. Jena, Phys. Rev. B **43**, 8179 (1991); K. Lee and J. Callaway, *ibid.* **49**, 13 906 (1994).

[5] B. V. Reddy, S. N. Khanna, and B. I. Dunlap, Phys. Rev. Lett. **70**, 3323 (1993).

[6] A. J. Cox, J. G. Louderback, and L. A. Bloomfield, Phys. Rev. Lett. **71**, 923 (1993); A. J. Cox, J. G. Louderback, S. E. Aspeal, and L. A. Bloomfield, Phys. Rev. B **49**, 12 295 (1994).

[7] Y. Jinlong, F. Toigo, and W. Kelin, Phys. Rev. B **50**, 7915 (1994); Y. Jinlong, X. Chuanyun, X. Shangda, and W. Kelin, *ibid.* **48**, 8253 (1993).

[8] S. K. Nayak, S. E. Weber, P. Jena, K. Wildberger, R. Zeller, P. H. Dederichs, V. S. Stepanyk, and W. Hergert, Phys. Rev. B **56**, 8849 (1997).

[9] C. H. Chien, E. Blaisten-Barojas, and M. R. Pederson (private communication).

[10] DMOL code, Biosym Technologies, Inc., San Diego, California.

[11] *Gaussian 94, Revision B.1*, edited by M. J. Frisch, G. W. Trucks, H. B. Schlegel, P. M. W. Gill, B. G. Johnson, M. A. Robb, J. R. Cheeseman, T. Keith, G. A. Petersson, J. A. Montgomery, K. Raghavachari, M. A. Al-Laham, V. G. Zakrzewski, J. V. Ortiz, J. B. Foresman, J. Closlowski, B. B. Stefanov, A. Nanayakkara, M. Challacombe, C. Y. Peng, P. Y. Ayala, W. Chen, M. W. Wong, J. L. Andres, E. S. Replogle, R. Gomperts, R. L. Martin, D. J. Fox, J. S. Binkley, D. J. Defrees, J. Baker, J. P. Stewart, M. Heads-Gordon, C. Gonzalez, and J. A. Pople (Gaussian, Inc., Pittsburgh, Pennsylvania, 1995).

[12] P. J. Hay, and W. R. Wadt, J. Chem. Phys. **82**, 299 (1985).

[13] S. H. Vosko, L. Wilk, and M. Nusair, Can. J. Phys. **58**, 1200 (1980).

[14] J. P. Perdew and Y. Wang, Phys. Rev. B **45**, 13 244 (1992).

[15] S. K. Nayak, S. N. Khanna, B. K. Rao, and P. Jena, J. Phys. Chem. A **101**, 1072 (1997).

[16] J. Guevara, A. M. Llois, and M. Weissmann, Phys. Rev. B **52**, 11 509 (1995).

[17] M. P. Allen and D. J. Tildsley, *Computer Simulation of Liquids* (Clarendon, Oxford, 1987).

[18] I. Shim, Mat. Fys. Medd. K. Dan. Vidensk. Selsk. **41**, 147 (1985).

[19] K. Balasubramanian and D. W. Liao, J. Phys. Chem. **93**, 3989 (1989).

[20] F. Illas, J. Rubio, J. Canellas, and J. M. Ricart, J. Chem. Phys. **93**, 2603 (1990).

[21] M. Harada and H. Dexpert, J. Phys. Chem. **100**, 565 (1996).

[22] K. A. Gingerich and D. L. Cocke, J. Chem. Soc. Chem. Commun. **1**, 536 (1972).

[23] H. Wang, H. Haouari, R. Craig, Y. Liu, J. R. Lombardi, and S. M. Lindsay, J. Chem. Phys. **106**, 2101 (1997).

[24] K. K. Das and K. Balasubramanian, J. Chem. Phys. **93**, 625 (1990).

[25] D. Dai and K. Balasubramanian, Chem. Phys. Lett. **195**, 207 (1992).

[26] P. Jena, B. K. Rao, and R. M. Nieminen, Solid State Commun. **59**, 509 (1986).

[27] B. V. Reddy, S. Nayak, S. N. Khanna, B. K. Rao, and P. Jena, J. Chem. Phys. **102**, 1748 (1998).

[28] B. I. Dunlap, Phys. Rev. A **41**, 5691 (1990).

[29] I. M. L. Billas, J. A. Becker, A. Châtelain, and W. A. de Heer, Phys. Rev. Lett. **71**, 4067 (1993).